International Journal of Applied Engineering Research ISSN 0973-4562 Volume 13, Number 1 (2018) pp. 30-39

Experimental and Numerical Hydrodynamic Analysis of a Planing Hull Pleasure Boat

Filippo Cucinotta*[1], Felice Sfravara[2]

Department of Engineering, University of Messina, Contrada Di Dio (S. Agata), 98166 Messina, Italy.

*(*Corresponding author)*

[1]Orcid: 0000-0002-0304-4004, Scopus ID 57192216810
[2]Orcid: 0000-0003-3922-8494, Scopus ID 57192214583

Abstract

The work addresses a critical analysis on the hydrodynamic of a high speed planing hull by carrying out towing tank tests and URANSe campaign. Towing tank tests have been performed by ITTC'57 standards. Computational Fluid Dynamics (CFD) has been solved by using an overset block, in order to avoid the morphing grid, during 2 degree of freedom motions.

Numerical results have matched experimental data with high accordance and allow to obtain crucial information that the tests in a model basin can hardly provide, as, for example, the true wetted surface in planing phase. A critical discussion of the results has been performed.

Keywords: Ship hydrodynamics; Towing tank test; CFD simulation; Overset grid; Hull design

INTRODUCTION

The main goal of each naval architect is to find the better solution in order to reduce the drag resistance of the ship during the navigation. In the last years the increase of the interest for the environmental impacts and the safety during the navigation [1] led the researchers to find new ways for studying the entire life of a product from cradle to grave. This is possible with the use of a Life Cycle Assessment (LCA); an example in mechanical industry is proposed by Barone et al. [2] with the application of the LCA for utility poles manufactured in different materials used for street lighting. In the naval field a cradle to grave analysis of a yacht manufactured in composite material [3] with two different process: hand lay-up and vacuum infusion, has been made by Cucinotta et al. [4], in this case the results highlighted the influence of different manufacturing processes in the final environmental impacts of the same product. Another way is to reduce the environmental impact reducing the power requested during the use life of the product. In the naval field, there are different ways for reducing this resistance, and the engineers can set in on the pressure component of resistance with the hull shape optimization or with new solutions for the reduction of the frictional component of resistance. In the first case the use of the computing power and numerical approach is fundamental in order to know in design phase the pressure component of resistance. There are many solutions and different numerical approaches for reaching this goal. An approach with simplified numerical simulation (BEM - Bounday Element methods) and the use of the T-Splines has been proposed by Kostas et al. [5] or as proposed by Han et al. the use of a parametric 3D hull shape surface generated by B-Spline labeled F-Splines [6]. Another approach is the use of CFD software with the use of Finite Volume methods, in this type of approach an useful tools are open-source programs because they allow to saving costs. A brief explanation of the potentiality of the open-source software is shown by Cella et al. [7] with the application of a loop of optimization for a catamaran sailing boat. Lombardi et al. [8] proposed a numerical tool for prediction and optimization of performance of a sailing yacht with the application of open-source library. Another way is to reduce the frictional component of resistance of the ship with active methods as the injection of the air under the hull. In this case is possible to use air layers or bubbles. Cucinotta et al. [9] proposed different design shapes for a planing boat for reducing the frictional component of resistance with the injection of air. Mitsubishi industries proposed a new method for injecting air under bulk carrier ships with the use of bubbles technology obtaining good results for drag reduction [10]. In these cases the numerical approach must be oriented to a good simulation of the interface air-water and in the capacity to capture the real shape of the air layer under the hull or the real shape of the bubbles. In this sense, thanks to commercial software, is possible to simulate the rising air bubble inside a column of water [11] or it is possible to predict, with the CFD application, the behaviour of the air layer injection along the bottom of a flat plate [12]. For each case, is fundamental to use a numerical approach in order to find the better solution in preliminary phase without using the experimental tests in towing tanks considering that they are too expansive. The paper shows, with all setting, a numerical procedure, validated with experimental tests in towing tank, for predicting the total resistance of a planing boat, the trim and sinkage position and finally the wetted surface by the water with the increase of velocity. The procedure uses an overset method for taking in account the motion of the boat during the planing condition. All the results have been compared with the experimental ones.

[1] Corresponding author.
[2] Corresponding author.

NOMENCLATURE

Definition	Symbol	Unit
Overall Length	LOA	m
Waterline Length	LWL	m
Waterline Beam	BWL	m
Static wetted Surface	S	m^2
Draft	T	m
Displacement	Δ	t
Displacement volume	∇	m^3
Longitudinal centre of gravity	x_G	m
Velocity	V	m/s
Drag resistance	R	N
Froude number	Fn	-
Reynolds number	Rn	-
Trim angle	τ	deg
Scale factor	λ	-

The subscript M refers to the model and the subscript S to the ship.

MATERIALS AND METHODS

Theoretical background

The first objective of a naval architect is to know, in preliminary phase, the resistance of the ship during the navigation to a specified velocity condition. In order to obtain this quantity, the engineer must know the physic principle of the fluid dynamics around the ship. The start point of each consideration are two simple physical concepts applied to an infinitesimal incompressible fluid element: the conservation of mass and the Newton's second law. Inside an infinitesimal element the total net transport of mass out of element have to be zero in absence of sources inside the element (Eq. 3.1 – Continuity Equation).

$$\frac{\partial u}{\partial x}+\frac{\partial v}{\partial y}+\frac{\partial w}{\partial z}=0 \tag{3.1}$$

The Newton's second law (Eq. 3.2) starts with a simple equation:

$$\overrightarrow{dF}=dm\,\vec{a} \tag{3.2}$$

A physical consideration is that in a fluid mechanic problem three different types of forces must be considered: body forces $\overrightarrow{dF_b}$, viscous forces $\overrightarrow{dF_v}$ and pressure forces $\overrightarrow{dF_p}$. Considering a coordinate system with the z-axis along the direction of the gravity, the only body force needs to be considered is the gravity force (Eq.4.3).

$$\frac{dF_{bz}}{dm}=-g \tag{3.3}$$

The pressure forces depend by the gradient of the pressure along all directions inside the infinitesimal element (Eq. 3.4-3.5-3.6).

$$\frac{dF_{px}}{dm}=-\frac{1}{\rho}\frac{\partial p}{\partial x} \tag{3.4}$$

$$\frac{dF_{py}}{dm}=-\frac{1}{\rho}\frac{\partial p}{\partial y} \tag{3.5}$$

$$\frac{dF_{pz}}{dm}=-\frac{1}{\rho}\frac{\partial p}{\partial z} \tag{3.6}$$

The viscous forces depend by the stresses inside the infinitesimal element, there are tangential viscous stresses and normal viscous stresses. The sum of each component of stress along respectively x-y-z direction defines the total viscous force along that direction (Eq. 3.7-3.8-3.9).

$$\frac{dF_{vx}}{dm}=\frac{1}{\rho}\left[\frac{\partial \sigma_{xx}}{\partial x}+\frac{\partial \sigma_{yx}}{\partial y}+\frac{\partial \sigma_{zx}}{\partial z}\right] \tag{3.7}$$

$$\frac{dF_{vy}}{dm}=\frac{1}{\rho}\left[\frac{\partial \sigma_{xy}}{\partial x}+\frac{\partial \sigma_{yy}}{\partial y}+\frac{\partial \sigma_{zy}}{\partial z}\right] \tag{3.8}$$

$$\frac{dF_{vy}}{dm}=\frac{1}{\rho}\left[\frac{\partial \sigma_{xz}}{\partial x}+\frac{\partial \sigma_{yz}}{\partial y}+\frac{\partial \sigma_{zz}}{\partial z}\right] \tag{3.9}$$

The principal hypothesis to the base of the Navier Stokes equation is the one defined by Newton. The stress components σ_{ij} are proportional to the rate of strain tensor (Eq. 3.10) with constant of proportionality the dynamic viscosity μ (Eq. 3.11). This correlation allows to define the stress components in function of the velocities.

$$S_{ij}=\frac{\partial u_i}{\partial x_j}+\frac{\partial u_j}{\partial x_i} \tag{3.10}$$

$$\sigma_{ij}=\mu\, S_{ij} \tag{3.11}$$

All these considerations lead to the Navier Stokes equations, a second order nonlinear system of differential equations (Eq. 3.12-3.13-3.14) and the continuity equation (Eq. 3.15). The entire system is a set of four equations that together constitute

a closed system for the four unknown variables: Pressure (*p*), vector velocity (*u,v,w*).

$$\frac{\partial u}{\partial t}+u\frac{\partial u}{\partial x}+v\frac{\partial u}{\partial y}+w\frac{\partial u}{\partial z} = -\frac{1}{\rho}\frac{\partial p}{\partial x}+\nu\left(\frac{\partial^2 u}{\partial x^2}+\frac{\partial^2 u}{\partial y^2}+\frac{\partial^2 u}{\partial z^2}\right) \quad (3.12)$$

$$\frac{\partial v}{\partial t}+u\frac{\partial v}{\partial x}+v\frac{\partial v}{\partial y}+w\frac{\partial v}{\partial z} = -\frac{1}{\rho}\frac{\partial p}{\partial y}+\nu\left(\frac{\partial^2 v}{\partial x^2}+\frac{\partial^2 v}{\partial y^2}+\frac{\partial^2 v}{\partial z^2}\right) \quad (3.13)$$

$$\frac{\partial w}{\partial t}+u\frac{\partial w}{\partial x}+v\frac{\partial w}{\partial y}+w\frac{\partial w}{\partial z} = -\frac{1}{\rho}\frac{\partial p}{\partial z}-g +\nu\left(\frac{\partial^2 w}{\partial x^2}+\frac{\partial^2 w}{\partial y^2}+\frac{\partial^2 w}{\partial z^2}\right) \quad (3.14)$$

$$\frac{\partial u}{\partial x}+\frac{\partial v}{\partial y}+\frac{\partial w}{\partial z}=0 \quad (3.15)$$

The system of Navier Stokes equation is elliptical with partial differential equations, this means that each boundary in the domain must have an initial condition. The domain around the ship has different boundaries: the hull surface, the free surface and the domain far from the hull. For each of these boundaries a condition must be imposed. On the hull surface, the so called no-slip condition have to be imposed (Eq. 3.16). This condition is relative to the components of velocity:

$$u=v=w=0 \quad (3.16)$$

On the free surface, where there are two phases in contact, liquid and gas, two different boundary conditions have to be defined.

The first one is a dynamic condition that expressing that the two phases on this surface must have the same velocities. This condition is imposed with the equality of the forces of the two phases. The equations 3.16-3.17 define the equality between the tangential components (*s,t*) for the water (*w*) and for the air (*a*).

$$\sigma_{(ns)_w}=\sigma_{(ns)_a} \quad (3.16)$$

$$\sigma_{(nt)_w}=\sigma_{(nt)_a} \quad (3.17)$$

In the case of the normal component (Eq. 3.18) of the force respect to the free surface, must be taken in account the effect of the surface tension (Δp_γ).

$$(\sigma_{(nn)}-p)_w=(\sigma_{(nn)}-p)_a+\Delta p_\gamma \quad (3.18)$$

The second one is a kinematic boundary that expressing the no flow through the surface. In this case the condition is that the vertical component of the velocity *w* must be equal to the derivative of the wave height respect the time (Eq. 3.19)

$$w=\frac{d\zeta}{dt} \quad (3.19)$$

Another important condition is the one to infinity. The extension of the domain is not limited. All disturbances have to go zero far from the hull surface.

There are two principal ways to solve the problem of resistance prediction of ship: experimental methods and numerical methods. The work proposed in this research uses the experimental techniques in order to obtain the resistance of the model proposed. Thanks to results from these techniques, a numerical approach has been investigated and validated for the model.

Experimental tests

If the variables inside the system of differential equations and in the boundary conditions are made dimensionless, the result is a system of differential equations governed by four dimensionless parameters: the Reynolds number (*Rn*), the Froude Number (*Fn*), the Weber (*Wn*) number and the Euler number (*En*). This transformation of the Navier-Stokes equations is explained by White [13].

The Reynolds number (Eq.4.1) is a parameter that allows to take in account the effects of the viscosity of the fluid. It is directly inside the equations of Navier Stokes. The Froude number (Eq.4.2) is a parameter that allows to take in account the effects of the gravity on the free surface, it appears inside the dynamic boundary condition on the free surface. The Weber number (Eq. 4.3) is a parameter that allows to take in account the surface tension effects, with particular interest on the spray and breaking waves. The Euler number (Eq.4.4) is a parameter that allows to take in account the effects of cavitation, this number is important only for cases where there is cavitation conditions.

$$Rn=\frac{VL}{\nu} \quad Eq.(4.1)$$

$$Fn=\frac{V}{\sqrt{gL}} \quad Eq.(4.2)$$

$$Wn=\frac{\rho V^2 L}{\gamma} \quad Eq.(4.3)$$

$$En=\frac{p_a}{\rho V^2} \quad Eq\ (4.4)$$

The sufficient and necessary condition for flow similarity between geosim bodies (two bodies with the same shape) at different scales is the condition of constancy of these four parameters [14]. If the above parameters are unchanged between two geosim bodies, the solution in no dimensional form is unchanged.

Inside the towing tank, by definition, the model has a length smaller than that of the ship, in order to keep all parameters equal to real scale the model speed should be adjusted and it is not possible to keep the four parameters at the same time equal. For example, in order to keep the same Froude number the velocity of the model has to be smaller than of that of the full scale, contrarily for the consistence of the Reynolds number or Weber number the velocity has to be higher. Only one parameter at a time can be maintained equal to real scale and the other three have to be sacrificed.

The Euler number concerns cavitation problems, usually in the flow around the hull no cavitation problem are found and it is possible to sacrifice this parameter. The Weber number governs the spray and the surface tension effects, they have a little effect on the total of resistance and this number can be sacrificed [14]. The choice is reduced between two parameters, the Reynold number and the Froude number.

Thanks to the studies of Froude [15], the approach for calculating the resistance of the ship in experimental way is based on an important concept: the possibility to split the resistance or the total coefficient of resistance (Eq. 4.5) in two independent parts (Eq. 4.6) governed by the Froude number (residuary part - C_R) and the Reynolds number (frictional part C_F).

$$C_T = \frac{R_T}{1/2\rho S V^2} \qquad Eq.(4.5)$$

$$C_T = C_F(Rn) + C_R(Fn) \qquad Eq.(4.6)$$

In the towing tank is conducted the test with a geosim model to the same Froude number of the hull at full scale. In order to have the same Froude number, the velocities to model scale and full scale must be defined by the equation:

$$V_M = V_S \sqrt{\frac{L_M}{L_S}} \qquad Eq.(4.7)$$

The test in the towing tank allows to obtain the total resistance of the model and so the total coefficient of resistance C_{TM}. The second step is to use the ITTC'57 formula in order to find the frictional component of the model (Eq.4.8). In this equation the number of Reynolds is the one in model scale. With the Equations. 4.9-4.10 is possible to find the total resistance coefficient of the ship.

$$C_{FM} = \frac{0.075}{(\log Rn_M - 2)^2} \qquad Eq.(4.8)$$

$$C_{RM} = C_{TM} - C_{FM} = C_{RS} \qquad Eq.(4.9)$$

$$C_{TS} = C_{RS} + \frac{0.075}{(\log Rn_S - 2)^2} \qquad Eq.(4.10)$$

The ship under investigation is a planing pleasure boat with the principal dimensions reported in Table 1.

Table 1: Principal dimensions of the ship

Symbol	Ship	Unit
LOA	18.0	m
LWL	14.9	m
BWL	4.3	m
T	0.945	m
Δ	30.5	t
S	66.2	m^2
x_G (% of LOA)	35.18 %	-

The range of the velocities of the real yacht are between the 12 knots and 32 knots, as shown in Table 2.

Table 2: Range of velocities for the yacht

V_S (m/s)	V_S (kts)	Fn
6.17	12.0	0.510
7.71	15.0	0.638
9.26	18.0	0.765
10.80	21.0	0.893
12.34	24.0	1.020
13.89	27.0	1.148
15.43	30.0	1.275
16.46	32.0	1.360

The tests inside the towing tank have to be conducted to the same Froude number of the ship, with a scaled geosim model, in order to apply the procedure above explained. The maximum velocity of the sip is 32 knots (16.46 m/s) and with a scale model of 6, and keeping the same Froude number the maximum velocity (Eq.4.7) for the model is 6.72 m/s. This velocity is inside the range of the towing tank possibility. In Table 3 are shown the eight velocities tested in the towing tank.

Table 3: Series of velocities

V_M (m/s)	Fn
2.520	0.510
3.150	0.638
3.780	0.765
4.410	0.893
5.040	1.020
5.670	1.148
6.300	1.275
6.720	1.360

Thanks to the towing tank results is possible to evaluate the resistance curve of the model and the relative position of the model respect to the free surface during the navigation. These results are useful in order to validate a numerical approach.

NUMERICAL APPROACH METHOD

For complex phenomena, the Navier Stokes equations have to be solved with a numerical approach because there is not an analytical solution. With the increase of the computing power, the research has been oriented in order to solve this set of equations with robust discretization methods [16]. In this study, a Finite Volume Method, implemented in a commercial software (Ansys Fluent 16.2) is used in order to evaluate the best modelling suitable for this kind of problem. The URANS equations are solved exploiting an implicit solver. A segregated flow approach has been used in order to solve the pressure and velocity fields; a predictor-corrector method [17] achieves to link the momentum and continuity equations. The most suitable turbulence model for planing hull is the k-omega SST Menter [18, 19], thanks to its capability to describe rapid changes of pressure. The process of discretization has been obtained with an Algebraic Multigrid method [20]. A blending method between the Gauss and Least Square method called Gauss-Least Square (Gauss-LSQ) allowed solving all the gradients during the process of discretization. Each simulation was an unsteady model with a 2nd order temporal discretization. The size of the time step (Δ_t) is influenced by the length and velocity of the ship, according to the ITTC equation 6.1 [21] and by the cell dimension, described by the Courant Number.

$$\Delta_t = 0.01 \sim 0.005 \frac{l}{v} \qquad (6.1)$$

For planing hulls, and in particular for the wave drag and spray evaluation, the choice of the interface tracking method is crucial. The more suitable model for solving the volume fraction, is the Volume of Fluid method (VoF). The HRIC (High-Resolution Interface Capturing) convection scheme has been used. It allows to keep always a sharp interface between the two immiscible fluids. The planing hull had 2 degree of freedom: pitch and heave motions. The Dynamic Body interaction solver has been activated. This is necessary to evaluate the hydrodynamic forces for forecasting the dynamic sinkage and trim of the hull. A minimum of 10 iterations are necessary to reach the equilibrium position of the ship, for each time step. The mesh change, in consequence of the ship motion, has been managed with the overset technique, that, for rapid and high movements, is better than morphing, as described by De Marco et al. [22]. Thanks to this methodology, the quality of cell elements is preserved, mainly when the trim angles are high. A linear interpolation scheme has been used for linking the solution between the background region and the overset one. In order to use the overset procedure, two different blocks of mesh has been defined inside the domain. The background block is the one fixed in the space and without motion. The overset block is the one with rigid body motion (Figure 1).

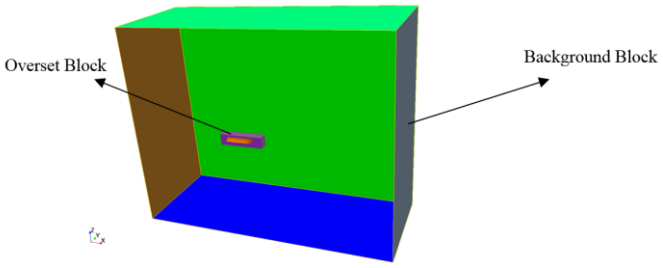

Figure 1: Overset block and Background Block

In the background block there are three different refinement mesh zones, one for capturing the free-surface interface, a second one for capturing the wave propagation (trinagular shape) and the last one in order to have the same element inside the zone of overlapping with the overset block.

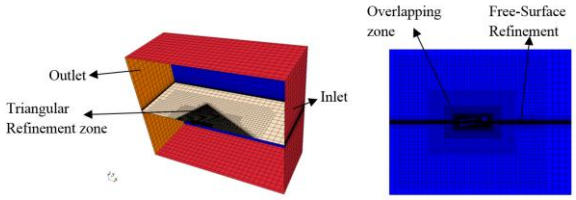

Figure 2: Refinement mesh zones for Background Block

In the overset block there is a refinement mesh zone for capturing the free-surface and another one for the hull surface.

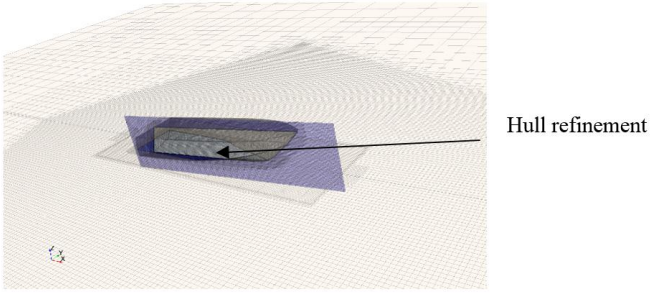

Figure 3: Overset zone

In the Figure 4 are shown two different position conditions of the ship, on left the starting point, on right the stable condition. In these two pictures is possible to see the rigid motion of the overset block respect to the background block.

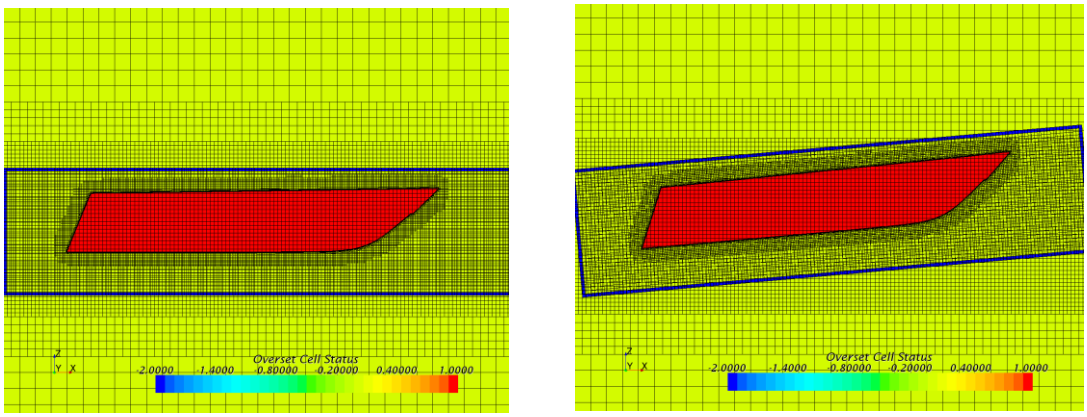

Figure 4: Overset motion

RESULTS AND DISCUSSION

During the experimental tests is possible to find three different parameters for each velocity. The resistance of the ship, the trim and sinkage position of the ship. In Figure 5 is shown the comparison between the drag curves obtained with experimental tests and the one obtained with numerical approach. The trend of the curve is the typical one of the planing boat, with an inflection in the zone of Froude number over 1 (starting of planing condition).

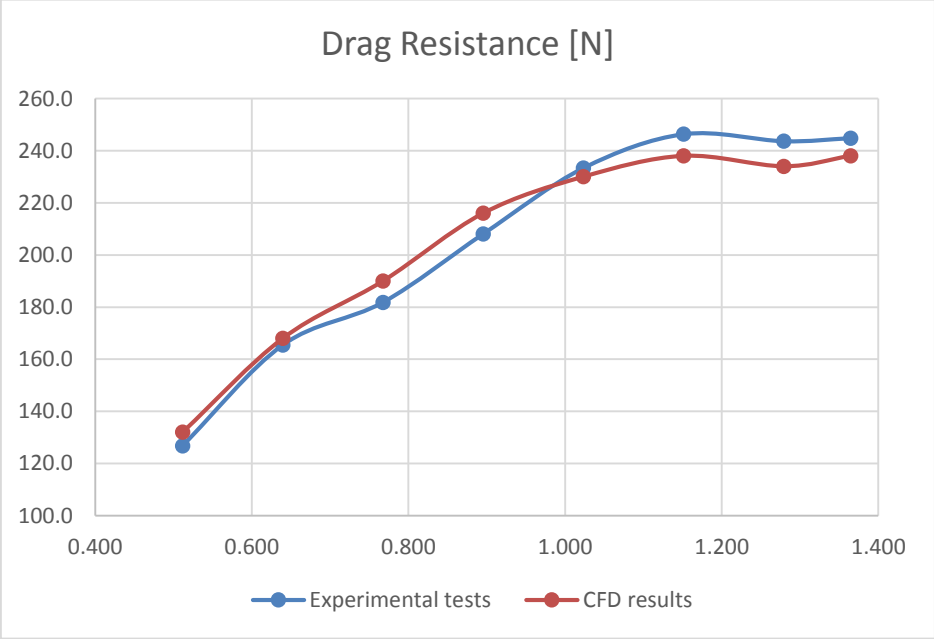

Figure 5: Drag resistance comparison

Table 4 Experimental and numerical results for drag resistance

V_M (m/s)	Fn	R_{MEXP}	R_{MCFD}	Abs Difference
2.520	0.510	126.8	132.0	4%
3.150	0.638	165.4	168.0	2%
3.780	0.765	181.8	190.0	4%
4.410	0.893	208.1	216.0	4%
5.040	1.020	233.3	230.0	1%
5.670	1.148	246.3	238.0	4%
6.300	1.275	243.7	234.0	4%
6.720	1.360	244.8	238.0	3%

Table 4 shows the results of the experimental tests and numerical simulations, the absolute difference between the two different methods is always under 5 %.

In the case of the rigid body motion (Table 5), the absolute difference for the trim angle reaches the maximum value of 11%. This difference is caused by the uncertainty of the position of the centre of gravity. Figure 6 shows the trim angle evolution.

Table 5: Experimental and numerical results for trim angle

V_M (m/s)	Fn	τ_{MEXP}	τ_{MCFD}	Abs Difference
2.520	0.510	2.66	2.55	-4%
3.150	0.638	3.94	3.60	-9%
3.780	0.765	4.23	4.500	6%
4.410	0.893	5.12	5.10	0%
5.040	1.020	6.13	5.60	-9%
5.670	1.148	6.50	6.10	-7%
6.300	1.275	5.99	5.40	-11%
6.720	1.360	5.71	5.20	-10%

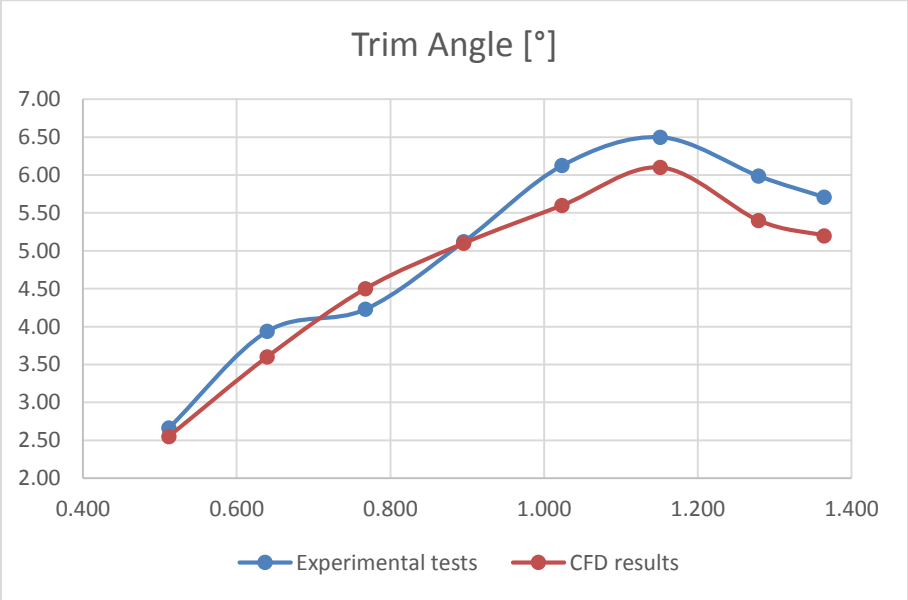

Figure 6: Trim comparison

Also for the case of sinkage (the relative movement of the ship in z-direction) there is a difference over the 10%. The influence of the centre of gravity is important also in this case.

Table 6: Experimental and numerical results for the Sinkage

V_M (m/s)	Fn	$Sinkage_{MEXP}$	$Sinkage_{MCFD}$	Abs Difference
2.520	0.510	56.6	52.0	-9%
3.150	0.638	65.8	61.0	-8%
3.780	0.765	54.3	46.3	-17%
4.410	0.893	46.3	42.0	-10%
5.040	1.020	40.6	36.0	-13%
5.670	1.148	26.0	23.0	-13%
6.300	1.275	8.3	7.2	-15%
6.720	1.360	-1.4	-1.3	-11%

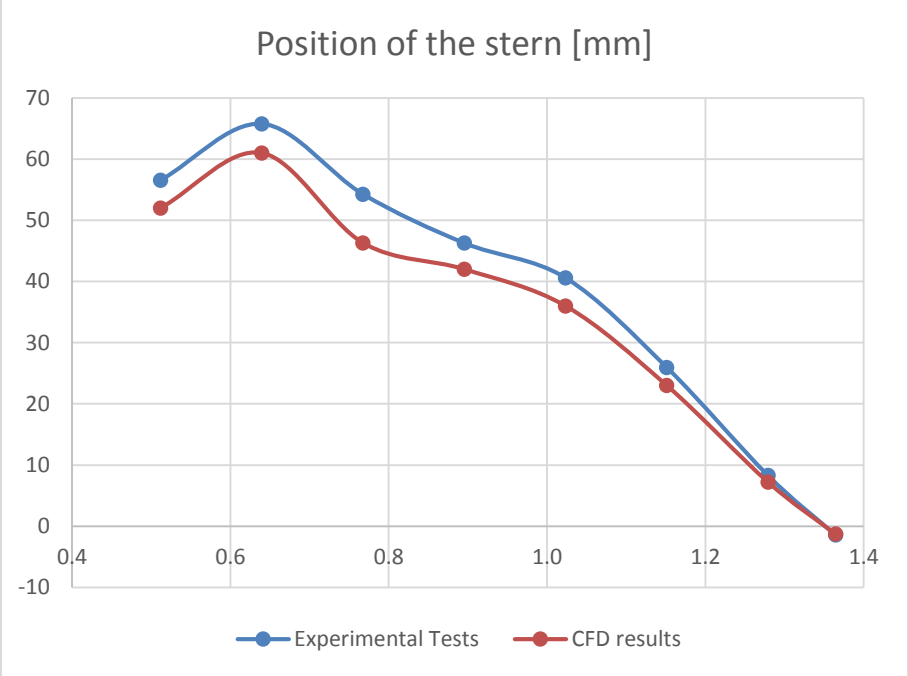

Figure 7: Sinkage comparison

Another important aspect evaluable with the numerical approach is the variation of the wetted surface during the increase of velocity. Usually, with experimental tests, this evaluation is hard to calculate or it is conducted with approximated methods. In the Figure 8 is shown the great difference between the static wetted surface (velocity of the ship equal to 0) and the dynamic wetted surface to the maximum velocity (6.72 m/s). The behaviour of this quantity during the increase of velocity is shown in Figure 9.

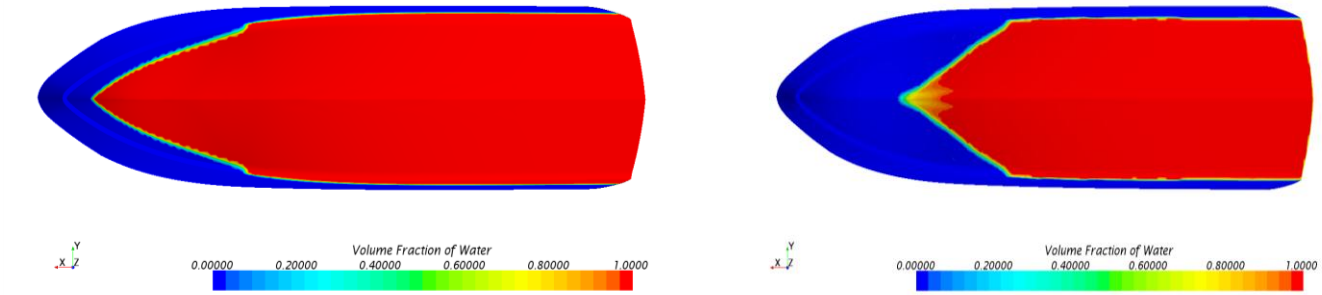

Figure 8: Volume fraction of water: on top V = 0 m/s; on bottom V = 6.72 m/s

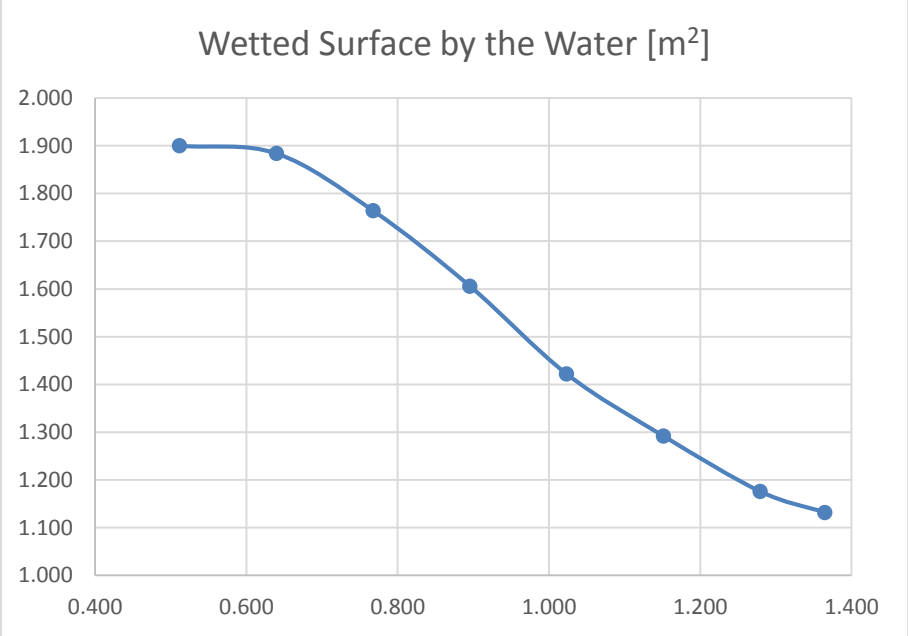

Figure 9: Wetted surface by the Water to different Froude numbers

CONCLUSIONS

Calm water resistance experiments have been conducted on a planing hull model with the ITTC'57 standards. An overset unsteady CFD UNRANSe campaign has been conducted. A comparison between experimental and numerical tests, in terms of drag resistance, trim and sinkage of the planing boat has been carried out. The founded accordance is very accurate, always under 5% in the drag and under 11% in the trim. By the evaluation of the numerical wetted surface it has been possible to obtain a parameter very useful for the prediction of the resistance of the ship in one-to-one scale, hardly evaluable by experimental testing.

REFERENCES

[1] Cucinotta F, Guglielmino E, Sfravara F (2017) Frequency of Ship Collisions in the Strait of Messina through Regulatory and Environmental Constraints Assessment. J Navig 1–21. doi: 10.1017/S0373463317000157

[2] Barone S, Cucinotta F, Sfravara F (2017) A comparative Life Cycle Assessment of utility poles manufactured with different materials and dimensions. In: Adv. Mech. Des. Eng. Manuf. pp 91–99

[3] Cucinotta F, Guglielmino E, Risitano G, Sfravara F (2016) Assessment of Damage Evolution in Sandwich Composite Material Subjected to Repeated Impacts by Means Optical Measurements. Procedia Struct Integr 2:3660–3667. doi: 10.1016/j.prostr.2016.06.455

[4] Cucinotta F, Guglielmino E, Sfravara F (2017) Life cycle assessment in yacht industry: A case study of comparison between hand lay-up and vacuum infusion. J Clean Prod 142:3822–3833. doi: 10.1016/j.jclepro.2016.10.080

[5] Kostas KV, Ginnis AI, Politis CG, Kaklis PD (2015) Ship-hull shape optimization with a T-spline based BEM–isogeometric solver. Comput Methods Appl Mech Eng 284:611–622. doi: 10.1016/j.cma.2014.10.030

[6] Han S, Lee Y-S, Choi YB (2012) Hydrodynamic hull form optimization using parametric models. J Mar Sci Technol 17:1–17. doi: 10.1007/s00773-011-0148-8

[7] Cella U, Cucinotta F, Sfravara F (2017) Sail Plan Parametric CAD Model for an A-Class Catamaran Numerical Optimization Procedure Using Open Source Tools. In: Lect. Notes Mech. Eng. Adv. Mech. Des. Eng. Manuf. pp 547–554

[8] Lombardi M, Parolini N, Quarteroni A, Rozza G (2012) Numerical Simulation of Sailing Boats: Dynamics, FSI, and Shape Optimization. pp 339–377

[9] Cucinotta F, Guglielmino E, Sfravara F (2017) An experimental comparison between different artificial air cavity designs for a planing hull. Ocean Eng 140:233–243. doi: 10.1016/j.oceaneng.2017.05.028

[10] Mizokami S, Kawakita C, Kodan Y, et al (2010) Experimental study of air lubrication method and verification of effects on actual hull by means of sea trial. Mitsubishi Heavy Ind Tech Rev 47:41–47.

[11] Cucinotta F, Nigrelli V, Sfravara F (2017) A preliminary method for the numerical prediction of the behavior of air bubbles in the design of Air Cavity Ships. pp 509–516

[12 Cucinotta F, Nigrelli V, Sfravara F (2017) Numerical prediction of ventilated planing flat plates for the design of Air Cavity Ships. Int J Interact Des Manuf. doi: 10.1007/s12008-017-0396-x

[13] White FM (2014) Fluid mechanics. doi: 10.1146/annurev.fluid.36.050802.122132

[14] Larsson L, Raven H (2010) The Principles of Naval Architecture Series: Ship Resistance and Flow. The Society of Naval Architects and Marine Engineers, New Jersey

[15] Froude W (1955) Observations and suggestions on the subject of determining by experiment the resistance of ships. Pap. William Froude

[16] Ferziger JH, Peric M (2002) Computational methods for Fluid Dynamics, 3rd Editio. Berlin, Heidelberg

[17] Deng Q-H, Tang G-F (2002) Special Treatment Of Pressure Correction Based On Continuity Conservation In A Pressure-Based Algorithm. Numer Heat Transf Part B Fundam 42:73–92. doi: 10.1080/10407790190053842

[18] Wilcox DC (2008) Formulation of the k-w Turbulence Model Revisited. AIAA J 46:2823–2838. doi: 10.2514/1.36541

[19] Menter FR, Kuntz M (2004) Adaptation of Eddy-Viscosity Turbulence Models to Unsteady Separated Flow Behind Vehicles. pp 339–352

[20] Stüben K (2001) A review of algebraic multigrid. J Comput Appl Math 128:281–309. doi: 10.1016/S0377-0427(00)00516-1

[21] ITTC (2011) Uncertainty Analysis in CFD Verification and Validation Methodology and Procedures.

[22] De Marco A, Mancini S, Miranda S, et al (2017) Experimental and numerical hydrodynamic analysis of a stepped planing hull. Appl Ocean Res 64:135–154. doi: 10.1016/j.apor.2017.02.004